

Network properties of healthy and Alzheimer's brains

José C. P. Coninck¹ · Fabiano A. S. Ferrari² · Adriane S. Reis³ · Kelly C. Iarosz⁴ · Antonio M. Batista⁵ · Ricardo L. Viana³

Received: date / Accepted: date

Abstract Small-world structures are often used to describe structural connections in the brain. In this work, we compare the structural connection of cortical areas of a healthy brain and a brain affected by Alzheimer's disease with artificial small-world networks. Based on statistics analysis, we demonstrate that similar small-world networks can be constructed using Newman-Watts procedure. The network quantifiers of both structural matrices are identified inside the probabilistic valley. Despite of similarities between structural connection matrices and sampled small-world networks, increased assortivity can be found in the Alzheimer brain. Our results indicate that network quantifiers can be helpful to identify abnormalities in real structural connection matrices.

Keywords Network · human brain · Alzheimer's disease · small-world

1 Introduction

One of the first fully reported neural network was the worm *C. elegans* (White et al., 1986). The nervous system of *C. elegans* consists of 302 neurons connected through 5000 chemical and 600 electrical synapses. Watts and Strogatz showed that the *C. elegans* brain network can be described by a small-world network (Watts and Strogatz, 1998; Varshney et al., 2011). Small-world networks are characterized by high clustering and short average distance between nodes. They have been observed in brain networks of animals and humans (Sporns and Zwi, 2004; Bassett and Bullmore, 2006; Stam, 2014; Medina et al., 2008). Evidences of small-world properties can also be found in ensembles of neurons *in vitro* (Bettencourt et al., 2007). The small worldness of neuronal networks is hypothesized to be a consequence of optimization process associated with minimal wiring cost, robustness and balance between local processing and global integration (Reijneveld et al., 2007; Bullmore and Sporns, 2012).

Brain networks can be obtained in different levels, such as microscale, mesoscale, and macroscale (Sporns et al., 2005; Heuvel and Yeo 2017, 2017). Microscale is in the level of the neurons and synapses, macroscale is used to define brain regions and large-scale communication pathways. Mesoscale is an intermediate level between micro and macroscale, where connections between large portions of the neuronal system are defined. A simple example of mesoscale network is the mini-columns (Stoop et al., 2013).

Neuronal networks are defined into structural or functional (Bullmore and Bassett, 2011). Functional networks are based on EEG, MEG or fMRI measures (Stam and Straaten 2012). Functional networks of Alzheimer's patients present increased path length when compared with healthy subjects (Stam et al., 2007).

¹Technological University of Paraná
Department of Statistics
Curitiba, Brazil

²Federal University of the Valleys of Jequitinhonha and Mucuri,
Institute of Engineering, Science and Technology
Janaúba, Brazil

³Federal University of Paraná,
Department of Physics
Curitiba, Brazil

⁴University of São Paulo,
Institute of Physics
São Paulo, Brazil

⁵State University of Ponta Grossa,
Department of Mathematics and Statistics
Ponta Grossa, Brazil

Structural connections can be characterized by diffusion weighted magnetic resonance imaging (DW-MRI) and graph theory (Lo et al., 2010). DW-MRI analyzes water diffusion in white matter, and together with fiber tractography it can be used to identify structural connections in the brain (Medina et al., 2007). The structural connection matrices of macaque and cats exhibit a complex structure (Hilgetag et al., 2000). The presence of clusters and modular architecture in structural connection matrices are observed by means of cortical thickness measurements (Chen et al., 2008). Matrices with small-world properties and exponentially truncated power law distribution were also reported (Gong et al., 2008).

In humans, the structural connection matrix mediates several complex cognitive functions (Bressler, 1995). Abnormalities in structural networks were found in patients with psychiatric disorders and neurodegenerative diseases (Stam et al., 2007; He et al., 2008, 2009; Yao et al., 2010; Pol and Bullmore, 2013; Stam, 2014). Disconnection between frontal and temporal cortices were observed in patients with Schizophrenia (Friston and Frith, 1995; Zalesky et al., 2011). Hyperconnectivity in the frontal cortex were reported in patients with Autism (Courchesne and Pierce, 2005). Alzheimer’s patient showed increased path length and reduced global efficiency (Lo et al., 2010). The alterations in brain networks are good indicators that network properties can be used as biomarkers for clinical applications (Kaiser, 2011).

Using diffusion tensor tractography, Lo et al. (Lo et al., 2010) constructed structural connection matrices of the human brain of healthy and Alzheimer’s subjects. The network is divided in 78 areas according to the automated anatomic label template (Tzourio-Mazoyer et al., 2002). The connection between the areas are defined in terms of the number of fibers, that were obtained through fiber assignment by continuous tracking algorithm (Mori et al., 1999).

In this work, we analyze the network properties of one structural connection matrix related to a healthy subject and other related to a subject suffering of specific neurodegenerative disease (Alzheimer). We demonstrate that similar networks to these brain matrices can be constructed using Newman-Watts procedure.

In Section 2, we provide a brief discussion about the network representation of the connectome. In Section 3, we introduce basic quantities that can be used to quantify networks. In Section 4, we discuss the basic quantities of small-world networks in the light of statistical analyses. In Section 5, we compare the properties of human brain networks to small-world networks. In Section 6, we present our final remarks.

2 Methodology

2.1 Properties of networks

Networks properties provide information about segregation, integration and influence (Rubinov and Sporns, 2010; Sporns, 2013). Segregation properties are associated with the presence of clusters or modules and integration properties are related to the network ability to transmit information through its nodes. Segregation and integration are linked with the network features while influence focus on the node features providing information about the relevance of a node inside the network.

2.1.1 Eigenvalues of the adjacency matrix

The eigenvalues of the adjacency matrix A are obtained by solving the characteristic equation of A ,

$$\det(A - \lambda I) = 0, \quad (1)$$

where I is the identity matrix and the values of λ that satisfy Eq. (1) are the eigenvalues (Cvetkovic et al. 2008, 2008). If the network is symmetric, $A_{ij} = A_{ji}$, then all the eigenvalues are real.

2.1.2 Degree and node strength

Degree κ_i is the number of neighbors of a node i ,

$$\kappa_i = \sum_{j=1}^N A_{ij}, \quad (2)$$

where N is the network size. It is considered one of the simplest measures to provide information about the influence of the network. The degree distribution is used to differentiate regular networks from random networks.

For weighted networks (W_{ij}), the use of node strength s_i instead of degree κ_i may be more appropriated (Opsahl et al. 2010, 2010). Node strength s_i is defined as the sum of the node connections,

$$s_i = \sum_{j=1}^N W_{ij}. \quad (3)$$

2.1.3 Transitivity

Transitivity T , Also known as clustering, is a measure of the segregation of a network. The Transitivity T is a measure of the amount of clustering between the node i and its k_i neighbours, the maximum number of connections between i neighbors is $C_{\max(i)} = k_i(k_i - 1)/2$.

C_i is defined as the ration between the number of active connections over the maximum number of connections $C_{\max(i)}$. The Transitivity T is the average over all nodes of the network.

The transitivity shows the effective proportion of the triangulation formed between the sites as a measure of clustering capacity, $G(E, V)$. Then, T is calculated by the following proportional ratio

$$T = \frac{3\delta(G)}{\tau(G)}, \quad (4)$$

where $\delta(G)$ or the number of triangles in graph G and $\tau(G)$ to denote the number of triples in graph G (Schanck and Wagner, 2005).

One simple method is to use the arithmetic mean (Opsahl and Pazaransa, 2009). If the nodes i , j , and k are connected, forming a triplet, the value of the triplet is the arithmetic mean between W_{ij} and W_{jk} . A triplet is considered a close tripled when the nodes i , j , and k are all connected to each other.

2.1.4 Characteristic path length

Characteristic path length L measures the average of the shortest paths d_{ij} between all pairs of nodes in the network,

$$L = \frac{2}{N(N-1)} \sum_{i=1}^N \sum_{j=1}^N d_{ij}. \quad (5)$$

This quantity is used for weighted and unweighted networks, it provides information about the network integration. When dealing with diffusion process and weighted networks, to calculate the shortest paths d_{ij} the inverse of the node strength should be used (Opsahl et al. 2010). For example, if $W_{12} = 2$, then $d_{12} = 1/2$, this approach considers that the higher is the node strength the faster information can be diffused through it.

2.1.5 Modularity

Networks can be divided in two or more modules, the trivial solution is to divide them into two modules, where one module has one node and another module containing all the remaining nodes. Basically, the modular structure is defined for any network and the question is to know the best method to identify modules in complex networks. An optimized quantity to characterize the modularity Q was defined by Newman (Newman, 2006), that is given by

$$Q = \frac{1}{4m} \sum_{ij} \left(A_{ij} - \frac{k_i k_j}{2m} \right) (s_i s_j + 1), \quad (6)$$

where $m = 1/2 \sum_i k_i$, s_i , and s_j are indices that depend on the group. The network is divided in two groups, if

the site j belongs to group 1, then $s_j = 1$, if j belongs to group 2, then $s_j = -1$. Q can be either positive or negative, positive values indicate the possible presence of community structure.

2.1.6 Assortativity

Assortativity ASR is a measure of the tendency of high connected nodes to be connected to others of similar degree k (Foster et al., 2010). When high connected nodes are more often connected to low connected nodes, the network exhibits assortative mixing. To define assortativity it is necessary to define the remaining $q(k)$ and $p(k)$. The probability that a random node has a degree k is given by the degree distribution $p(k)$, however, the probability to select a random edge is not proportional to $p(k)$ but to $kp(k)$, because the most connected nodes receive more connections. Considering that node i is connected to node j through a random selected edge, the remaining degree is the number of nodes that leaves the node j , excluding node i . The normalized remaining degree distribution is given by

$$q(k) = \frac{(k+1)p(k)}{\sum_j jp(j)}. \quad (7)$$

The Assortativity ASR is defined as:

$$ASR = \frac{1}{\sigma_q^2} \sum_{ij} ij(e(i, j) - q(i)q(j)), \quad (8)$$

where σ_q^2 is the variance of the remaining degree and $e(i, j)$ is the joint probability distribution of the remaining degree of two nodes (Newman, 2002). The Assortativity A is defined in the interval $-1 \leq A \leq 1$, when $A = 1$ the network has perfect assortative mixed patterns, $A = 0$ indicates the network is not assortative and $A = -1$ means the network is completely dissortative.

2.2 Statistical analysis

2.2.1 Generalized regression analysis

A generalized linear model is made up of a combination of linear predictor with link function,

1. Predictor linear: $\eta_i = \beta_0 + \beta_1 x_{1i} + \beta_2 x_{2i} \cdots + \beta_p x_{pi}$
2. Link function: $g(\mu_i) = \eta$ for exponential family of distributions

$$f(y, \theta, \phi) = \exp \left\{ \frac{y\theta - b(\theta)}{\phi - c(y, \phi)} \right\},$$

with

$$\begin{cases} E(Y_i) = \mu_i = \frac{d[b(\theta_i)]}{d\theta} \\ Var(Y_i) = \phi^{-1} V_i \quad \phi^{-1} > 0. \\ V = \frac{d\mu}{d\theta} \end{cases}$$

2.2.2 Multivariate data analysis

Multivariate analysis is a branch of statistics that deals with the relationship between many variables, including the reduction of the number of variables observed during an experiment. The main tools for multivariate data analysis are principal component analysis (PCA) (Gray, 2017), factor analysis (Jhonson and Wischern, 1998), classifications (Jhonson and Wischern, 1998), structural equations models (SEM) (Grace, 2016; Maruyama, 1998), among other techniques. In our case, the multivariate analysis of the data is useful to vary the possible second order relationships between variables not directly correlated, such as transitivity, assortativeness and the modularity of the human network. At the end of this paper we will see how these measures are related using the SEM (Maruyama, 1998).

2.2.3 Development of a questionnaire

We apply a questionnaire to a population in the small-world models artificially generated with network size in 3 to 100 sites, from a single connection to the global connection. The determination of sample (Cochran, 1977)

$$n = \frac{\sum_{N=3}^{100} \sum_{k=1}^N \binom{N}{k} \hat{p}\hat{q}z_{\alpha/2}^2}{\hat{p}\hat{q}z_{\alpha/2}^2 + (\sum_{N=3}^{100} \sum_{k=1}^N \binom{N}{k} - 1)E^2}, \quad (9)$$

for optimization $\hat{p} = \hat{q} = \frac{1}{2}$, with error $E \approx \pm 3\%$ in $N = 2499$ population with $z_{\alpha/2}$ is a z-score distribution with level of significance $\alpha \approx 5\%$. In this case, the sample is $n \approx 492$ small-world models. This questionnaire is composed of 34 variables or questions about graph proprieties and applied to each small-world. Each model randomly generated with a certain probability is measured with these thirty-four variables.

We verify the quality of the questionnaire through Cronbach's alpha (Cronbach 1951, 1951)

$$\alpha = \frac{K}{K-1} \left(1 - \frac{\sum_i \sigma_{Y_i}^2}{\sigma_{X_i}^2} \right), \quad (10)$$

where K is the number of components, $\sigma_{X_i}^2$ is the variance of the observed total test scores, and $\sigma_{Y_i}^2$ is the variance of the current sample of generated small world. The questionnaire quality applied to small-world networks is equal to 0.89, indicating a good Internal consistency (Cronbach 1951, 1951; Maruyama, 1998).

The questionnaire is composed of thirty-four questions (or variables) measured directly in each artificial small-world network. Each variable measures an important network property and the comparison between the human network and the small-world model is given by

Table 1 Cronbachs alpha.

alpha	Internal consistency
$0.9 \leq \alpha$	Excellent
$0.8 \leq \alpha \leq 0.9$	Good
$0.7 \leq \alpha \leq 0.8$	Acceptable
$0.6 \leq \alpha \leq 0.7$	Questionable
$0.5 \leq \alpha \leq 0.6$	Poor
$\alpha < 0.5$	Unacceptable

means of these measures. The small global templates are generated with 10 sites up to 100 sites. Each generated model has different connections of its neighborhood between a single neighbor and the global network. This way, 492 samples of small-world models are produced. The measure of sampling adequacy (MSA) through the Kaiser-Meyer-Olkin (KMO) test indicates considered reasonable for value $KMO = 0.73$ (Kaiser, 1974). The KMO and RMSA measures are given by

$$KMO = \frac{\sum_{i=1}^k \sum_{j=1}^k r_{ij}}{\sum_{i=1}^k \sum_{j=1}^k r_{ij}^2 + a_{ij}^2}, \quad (11)$$

and

$$RMSA = \frac{\sum_{j=1}^k r_{ij}}{\sum_{j=1}^k r_{ij}^2 + a_{ij}^2}, \quad (12)$$

where r_{ij} is the correlation matrix term and a_{ij} is the anti-image-correlation matrix term. In this method, the inverse correlation matrix is close to the diagonal matrix. To verifies if matrix correlations is statistical equivalent to an identity matrix, we use the Bartlett's test. The basic hypothesis is that population's correlation matrix is an identity matrix equivalent. In our variables group, p-value $\ll 0.05$ implies the rejection of the null hypothesis and accepting the factorial analysis.

3 Results

3.1 Structural connection matrices

In this work, we use two structural connection matrices, one for the healthy brain (Fig. 1(a)) and other for the Alzheimer's brain (Fig. 1(b)) (Lo et al., 2010). Both networks are weighted and symmetric, the weight is associated with the intensity of connections and can assume five values: 0 (no connections, white region), 1 (low density of connections, indigo circles), 2 (intermediate density of connections, red circles), and 3 (high density of connections, orange circles). The main results for the networks are shown in Table 3. Figure 1 exhibits two adjacency matrix connection W_{ij} : (a) healthy brain and (b) Alzheimer's brain. The eigenvalues for these adjacency matrix are evaluated in Fig. 2. The healthy structural connection matrix is in black

Table 2 Variables of questionnaire - graph.

N :	Number of nodes
p :	Probability connection
DE :	Density edge
L :	Average path length
Rep :	Reciprocity
E :	Edges
N :	Vertices
NL :	number of links
NL_I :	Internal number of links
DL :	link Density
TST :	Total System Throughput
$TSFR$:	Total System Flow Rate
Cn :	Conectancie
ALW :	Average Link Weight
ACT :	Average Compartment Throughflow
Cp :	Compartmentalization
T :	Transitivity
ASR :	Assortivity
Ecc :	Eccentricity
D :	Diameter
I_{max} :	Maximum interweaving
I_{min} :	Minimum interweaving
Q :	Modularity
E :	Eficience
R :	Radius
K_{max} :	Max K-Core
K_{min} :	Min K-Core
K_{mean} :	Mean K-Core
Iso :	Isomorfism
$Auto$:	Automorphism
$EfcM$:	Number of edge with max efficiency
$Efcm$:	Number of edge with minimal efficiency
λ_p :	Principal eigenvalures
$detM$:	Determinant matrix

and Alzheimer's structural connection matrix is in red. The eigenvalue spectrum for small world with 78 nodes is $p = 0.0375$ (blue line). The ordinate eigenvalues are very close for three structures matrix. The eigenvalues are equivalent when there is some difference in the dispersion of adjacency matrix.

Table 3 Network Indicators (W:Weighted Un:Unweighted).

	Healthy		Alzheimer	
	W	Un	W	Un
Transitivity T	0.578	0.578	0.560	0.559
Assortivity ASR	0.081	0.010	0.226	0.125
Path Length L	2.248	2.248	2.281	2.281
Modularity M_1	0.451	0.423	0.483	0.428
σ	23.27	0.590	7.534	0.590
Average Degree	8.000	1.383	17.487	1.383

3.2 Small-world networks

A network with small-world properties can be generated by means of different methods (Newman, 2000). The most common method was developed by Watts and Strogatz (Newman, 2000), where the regular edges are replaced by random edges. When about 1% of the total edges are replaced, the network exhibits high transitivity and low path length (Watts and Strogatz, 1998). For our analysis, we consider an alternative method, where

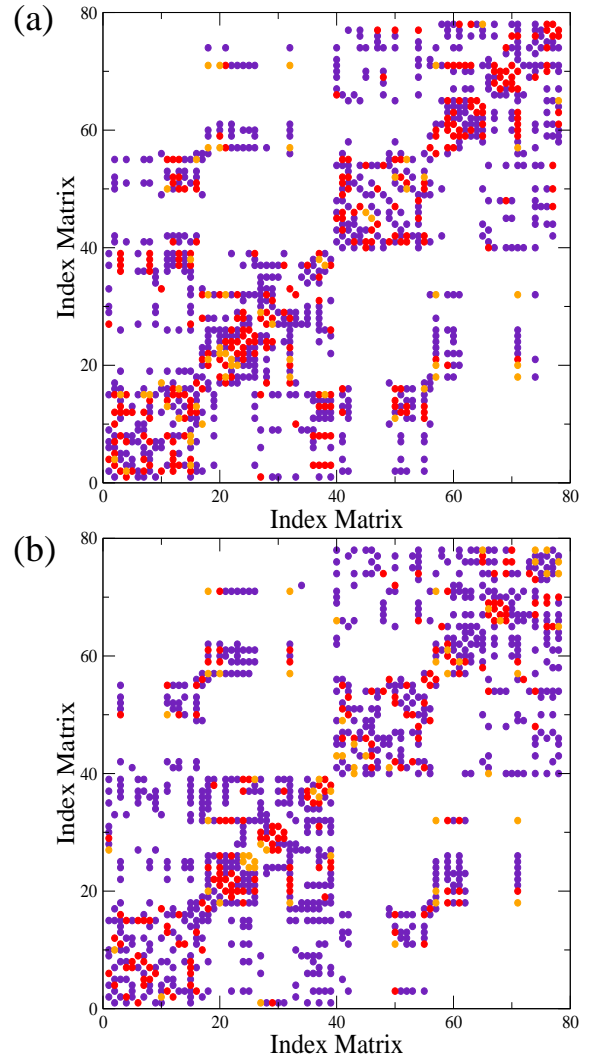


Fig. 1 Weighted connection matrix W_{ij} for (a) healthy and (b) Alzheimer's brains. The weight is associated with the intensity of connections: 0 (no connections, white region), 1 (low density of connections, indigo circles), 2 (intermediate density of connections, red circles), and 3 (high density of connections, orange circles).

instead of randomly replace regular edges by random edges, we only add random edges, known as Newman-Watts procedure (Newman, 2003). We add pNK new random edges, where N is the network size, K is the regular network degree, and p is the probability to add new edges. We vary p and identify the small-world properties comparing T and L with the values of the regular network $T(0)$ and $L(0)$. We find

– Healthy brain

$$DL : \text{link density} \longrightarrow \frac{DL}{2} = \frac{13.3333}{2} \approx 7, \quad (13)$$

– Alzheimer's brain

$$DL : \text{link density} \longrightarrow \frac{DL}{2} = \frac{13.38462}{2} \approx 7. \quad (14)$$

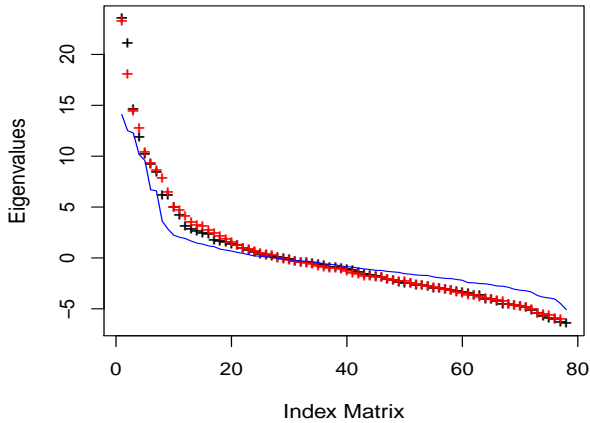


Fig. 2 Eigenvalue spectrum for the weighted matrices of Fig. 1. Healthy structural connection matrix is in black and Alzheimer's structural connection matrix is in red. Eigenvalue spectrum for small-world with 78 nodes and connection probability is $p = 0.0375$ in blue continue line.

The number of nodes in the human graph is 78 sites and the average degree is 7 neighbors per node. Due to this fact we create the equivalent connection network under these conditions to depend exclusively on the probability of calling. It is generated small-world graph with number of nodes $N = 78$, 7 neighbours per node, and without the likelihood of connection ($p = 0$), implying in average length $L_0 = 3.27273$ and transitivity $C_0 = 0.69231$. For healthy human structural connection matrix, we find $L_{\text{healthy human}} = 2.24875$ and $C_{\text{healthy human}} = 0.57813$. Then, we obtain

$$\frac{C_{\text{healthy human}}}{C_0} = 0.8350739, \quad (15)$$

$$\frac{L_{\text{healthy human}}}{L_0} = 0.6871175,$$

$$\Rightarrow \frac{C}{C_0} > \frac{L}{L_0},$$

$$\frac{C_{\text{Alzheimer's structural}}}{C_0} = 0.8087265,$$

$$\frac{L_{\text{Alzheimer's structural}}}{L_0} = 0.6971917,$$

$$\Rightarrow \frac{C}{C_0} > \frac{L}{L_0}.$$

C/C_0 is approximately 1.4% more than Alzheimer's disease human cluster standardized, and L/L_0 is approximately 3.1% less than Alzheimer's disease human. The propagated information in Alzheimer's disease human presents greater difficulty for diffusion of information in network, becoming more complex than healthy human matrix. Therefore, there seems to be a relation-

ship between the transfer of the network and its grouping, i.e., relations between assortivity, modularity and transitivity.

In correlation matrix, we present a statistical correlations r_{ij} for variables assortivity (ASR), modularity (Q), and transitivity (T), respectively, for small-world samples classes used in RMSA and KMO analysis. All values are low and indicate the lack of direct correlation.

3.2.1 Regression analysis

In a convenience sample, for $n = 429$ small-world type networks, five replicas are executed to create variation within the others. The dispersion of the transitivity according to the logarithm of the connection probability shows a decay adjusted by generalized model Gaussian family with link identity

$$f(y|\mu, \sigma^2) = \exp \left[\frac{1}{\sigma^2} \left(y\mu - \frac{\mu^2}{2} \right) + \left(-\frac{1}{2} \ln(2\pi\sigma^2) - \frac{y^2}{2\sigma^2} \right) \right],$$

resulting in the following regression

$$T_{SW} = 0.300314 - 0.029338 \ln p. \quad (16)$$

For instance, when the probability connection is $p = 0.00091188196$, then $\log p$ is equal to -7 . The result is approximately 0.50568. This probability value p is in agreement with the probability of small-world connection. When the connection probability increases, the dispersion of the transitivity value increases as well. On the other hand, the decrease in probability linkage causes the dispersion to become smaller and more concentrated, characterizing a good small-world region. $T_H = T_M = T_{SW}$ is valid for the small-world model. Another feature of Eq. 16 is its rate of transitivity in relation to the log of the probability,

$$\frac{dT_{SW}}{d \ln p} = -0.029338 \approx -3\%. \quad (17)$$

The ratio of transitivity to $\ln p$ is equal to the loss value in the small-world model when we compare the matrix of healthy human adjacency with disease Alzheimer human matrix.

The transfer rate and the rate of flow in the network with Alzheimer's exhibit a drop equal to that caused in the transitivity when compared with the human network in the normal state, as shown in Table 4. It suggests that the rate of transfer and rate of flow for people with Alzheimer's disease declines with 5.4%, possibly due to the fall in transitivity in 3.1%.

Table 4 Transitivity loss (weighted).

	Healthy	Alzheimer	loss
Transitivity	0.57813	0.5598876	3.1%
Nodes	78	78	
Links total	1040	1044	
Transfer rate	1438	1364	5.4%
Leak rate	1438	1364	5.4%

3.2.2 Assortativity

One of the most difficult measure to be statistically analyzed is the assortivity of the network. Due to the fact that the network topology of small-world is very sensitive to the probability of (re)connection. This can be verified in healthy and Alzheimer's human matrices. for $T = 0.57$, the assortivity shows very different values. However, the assortiveness is 2.5 times higher for the Alzheimer's brain than for healthy (Table 3).

The Alzheimer's brain is more assortive than the healthy brain, this means that in the Alzheimer network the nodes with high degree are, in average, connected with other nodes of high degree more intensely than the healthy human network. We calculate the assortativity distribution for small-world networks for $n = 492$ samples. In a sample, for example the small-world $N = 10$ and second order connection, the assortiveness presents an sample average of $\langle ASR \rangle = -0.01335938$ not being statistically zero according to t-Student test for the hypothesis $H_0 : \mu_{ASR} = 0$. There is no significant evidence to support the null hypothesis for a p-value $\ll 0.05$, inclining us to accept the hypothesis that assortiveness in the sample question is, in fact, negative. The network is on average disassortative. This does not imply the formation of positive assortiveness as verified in the graph.

3.2.3 Probabilistic valley

The probabilistic valley is a region where the small-world structure behaves by sequences of abrupt changes. It is precisely in this region that we identify abrupt behaviors of assortativeness, given the equivalent modularity and transitivity. These three measures of the small-world model that are equivalent to the measurements of the human matrix are found in this valley. The probabilistic voucher is developed through the structural equations model (SEM), in which it is related indirectly to assortivity, transitivity and modularity. As assortiveness represents the equivalent of the correlation between the links of the sites of a network, we write the assortivity in function of the transitivity and the modularity of the network for determinate probabilistic valley.

The probabilistic valley region indicates a possible existence of probability as a function of the modularity, transitivity and efficiency, that it is in agreement with the SEM analysis. This indicates that there is a possible dependence on the functions of modularity, assortiveness, transitivity and efficiency, according to the SEM analysis. In the same region random overflow occurs in assortivity increasing transitivity and modularity. The increase in assortivity and transitivity implies in the decay of the connection probability, which confirms that the probability value decreases. A more detailed view of the level curve with the modularity in the abscissa of the assortative at the ordinate reveals a complex structure of the curves. Outside this region the value of the assortiveness is zero or close to zero.

The valley has many interesting behavior. The assortivity, transitivity and modularity measures exist only because there are valley probabilistic. To generate Fig. 3, we consider a set of 100 independent models of small-world networks starting with 10 sites up to the amount 100 sites. In all models, we vary the probability of linkage between the non-coupling state ($p = 10^{-6}$) and the overall state ($p = 1$). The red dot in Fig. 3 is located in the region where the modularity (≈ 0.45) and transitivity (≈ 0.58) have values equal to the results found through the human matrix of healthy individuals. The same point coincides with the result of the assortiveness (≈ -0.02) in the Alzheimer's human matrix. This graph located in this point have 78 sites with 7 connections neighbors and probability range $8 \cdot 10^{-8} < p < 0.5$.

4 Discussion

The human networks are located in the probabilistic valley. We locate the healthy and Alzheimer's human networks within the small-world samples. The superposition both red and blue dots in evolutionary average length measures and transitivity graphics in connection probability is $p = 0.0375$, as shown by the vertical dotted line of Fig. 4. This ordered pair $\left(\frac{T}{T(0)}, \frac{L}{L(0)}\right) = (0.8350739, 0.6871175)$ for $p = 0.0375$ is exhibited by the blue dots in Fig. 4. The same technique is used to find the ordered pair representing Alzheimer's structural connection matrix for

$$\left(\frac{T}{T(0)}, \frac{L}{L(0)}\right) = (0.8087265, 0.6971917). \quad (18)$$

In this case, it is represented by the red dots in same figure.

In fact, when we select the region of the transitivity of Fig. 4 in the value of the probability of connection, we have that the difference between the blue and red

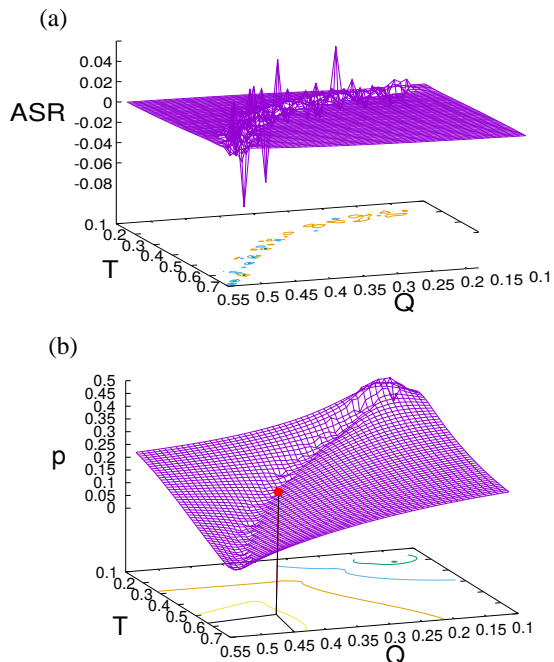


Fig. 3 Probabilistic valley as functions of modularity and transitivity for: (a) Assortivity and (b) probability of non-local connections.

points is 3.1%, which represents the healthy individual and Alzheimer's disease, respectively. The human Alzheimer's network exhibits greater difficulty in the transmission of information due to the fall of transitivity in the network. On the other hand, Fig. 4 also shows that the path length (L) is larger than the case of healthy individuals. The individuals with Alzheimer's disease have a decrease in the effectiveness of the transitivity.

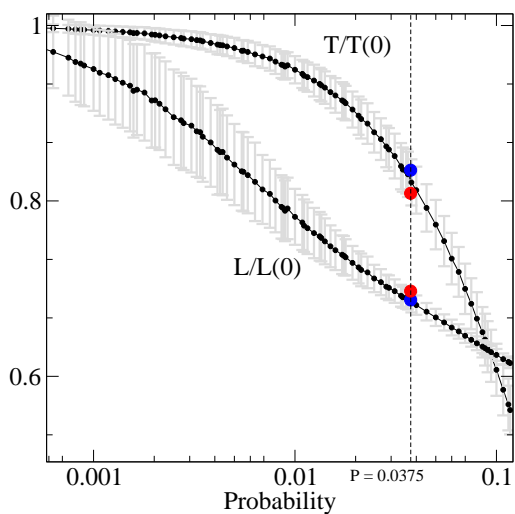


Fig. 4 $L/L(0)$ and $T/T(0)$ as a function of the probability. The results for healthy and Alzheimer's structural connection matrix are shown by blue and red balls, respectively.

The weighted connection matrix eigenvalues W_{ij} is useful for the comparison between the matrix structures. In Fig. 2, we display the eigenvalue spectrum for both networks of Fig. 4. We verify that the eigenvalues of both networks are similar. The eigenvalues of the proposed small-world model are very close to the human adjacency matrices. The approximation of the variation of the transitivity region in Fig. 4 can be seen in Fig. 5. This figure show us two points, one blue and another red that represent the health human and Alzheimer's disease, respectively. The difference between the the healthy and Alzheimer's brains is about 3.1%.

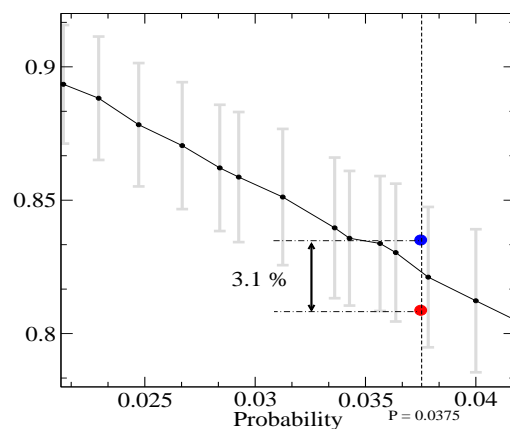


Fig. 5 Magnification of $T/T(0)$ as a function of the probability of Fig. 4.

Table 5 shows that the average path length value of the healthy brain is very close to small-world network. The transitivity, assortivity, eccentricity, and modularity are almost identical. In fact, the relationship between a human graph and a small-world structure is pertinent. In Table 6, we see that the Alzheimers's brain and small-world network have similar values, except the assortivity value, $\varepsilon = 59.62\%$.

Table 5 Values of the healthy brain and small-world network.

	Health human (real)	Small-world (Simulated)	error (ε)
Average path length	2.2487	2.1964	+2.32%
Density of links	13.333	14.000	-5.00%
Transitivity	0.5781	0.5386	+6.79%
Assortivity	0.0815	0.0882	-8.32%
Eccentricity	3.6667	3.5128	+4.20%
Modularity	0.4515	0.4889	-8.27%

Table 6 Values of the Alzheimer's brain and small-world network.

	Alzheimer's brain (real)	Small-world (Simulated)	error (ϵ)
Average path length	2.28172	2.1964	+3.74%
Density of links	13.3846	14.000	-4.59%
Transitivity	0.55989	0.5386	+3.80%
Assortivity	0.21846	0.0882	+59.62%
Eccentricity	3.76923	3.5128	+6.80%
Modularity	0.49083	0.4889	+0.39%

5 Conclusions

In this work, we show that small-world networks can be used to mimic brain networks. Comparing the healthy human matrices and the small-world model with probability of connection about 3.75%. It is evident the proximity of the measures indicators of the graphs, such as the average path length that presented 97% of proximity with the result of the human matrix.

We find a relation of construction among the variables associated with the transmission of information in the network, such as the transitivity (0.57813 for the healthy brain and 0.5386 for the small-world network), the assortivity (0.08151 for the healthy brain and 0.08829 for the small-world network), the eccentricity (3.66667 for the healthy brain and 3.51282 for the small-world network), and the modularity (0.45157 for the healthy brain and 0.48891 for the small-world network), whose values are very close to each other. In all four measures, we obtained errors (ϵ) smaller than 10% in the measurements up or down. This characteristic was verified in the variation of the transitivity and the length of the average path as a function of the probability. In both cases, the healthy human network and the human network for the Alzheimer's brain were within the simulated region for a small-world sample, thus indicating a close linkage probability of 3.75%. Exactly a small-world model in this region, for an equivalent assortiveness value, have very similar graph properties thus demonstrating that the human network (diseased or not) behave as a small-world network.

We verify that the healthy brain can be mimicked by networks with small-world properties. The network indicators of the Alzheimer's brain are almost identical with the small-world network, except the assortivity. Therefore, the assortivity could be a diagnostic tool to identify Alzheimer's brain.

Acknowledgements We wish to thank the Brazilian government agencies: Fundação Araucária, CNPq (420699/2018-0, 407543/2018-0), FAPESP (2015/50122-0, 2018/03211-6), and CAPES for partial financial support.

References

- Bassett DS and Bullmore E (2006) Small-World Brain Networks. *The Neuroscientist* 12:512-523.
- Bettencourt LMA, Stephens GJ, Ham MI and Gross GW (2007) Functional structure of cortical neuronal networks grown *in vitro*. *Phys. Rev. E* 75:021915.
- Bressler SL (1995) Large-scale cortical networks and cognition. *Brain Res. Rev.* 20:288-304.
- Bullmore ET and Bassett DS (2011) Brain graphs: graphical models of the human brain connectome. *Annu. Rev. Clin. Psycho.* 7:113-140.
- Bullmore E and Sporns O (2012) The economy of brain network organization. *Nat. Rev. Neurosci.* 13:336-349.
- Chen Z1, He Y, Rosa-Neto P, Germann J and Evans AC (2008) Revealing modular architecture of human brain structural networks by using cortical thickness from MRI. *Cereb. Cortex* 18:2374-2381.
- Cochran WG (1977). *Sampling Techniques*. John Wiley & Sons. ISBN-10:047116240X.
- Courchesne E and Pierce K (2005) Why the frontal cortex in autism might be talking only to itself: local over-connectivity but long-distance disconnection. *Curr. Opin. Neurobiol.* 15:225-230.
- Cronbach LJ (1951) *Psychometrika* 16:297. <https://doi.org/10.1007/BF02310555>
- Cvetković D, Rowlinson P and Simić S (1997) *Eigenspaces of graphs*. Cambridge University Press, Cambridge.
- Ferrari FAS, Viana RL, Reis AS, Iarosz KC, Caldas IL and Batista AM (2018) A network of networks model to study phase synchronization using structural connection matrix of human brain. *Physica A* 496:162170.
- Foster JG, Foster DV, Grassberger P and Paczuski M (2010) Edge direction and the structure of networks. *P. Natl. Acad. Sci. USA* 107:10815-10820.
- Friston KJ and Frith CD (1995) Schizophrenia: a disconnection syndrome? *Clin. Neurosci.* 3:89-97.
- Gone G, He Y, Conhca L, Lebel C, Grossa DW, Evans AC and Beaulieu C (2009) Mapping anatomical connectivity patterns of human cerebral cortex using *in vivo* diffusion tensor imaging tractography. *Cereb. Cortex* 19: 524-536.
- Grace JB (2006) *Structural Equation Modeling and Natural Systems*. Cambridge, UK: Cambridge University Press.
- Gray V (2017) *Principal Component Analysis: Methods, Applications, and Technology*. Hauppauge, New York: Nova Science Publishers, Inc (Mathematics Research Developments).

- He Y, Chen Z and Evans A (2008) Structural Insights into Aberrant Topological Patterns of Large-Scale Cortical Networks in Alzheimers Disease. *J. Neurosci.* 28:4756-4766.
- He Y, Dagher A, Chen Z, Charil A, Zijdenbos A, Worsley K and Evans A (2009) Impaired small-world efficiency in structural cortical networks in multiple sclerosis associated with white matter lesion load. *Brain* 132:3366-3379.
- van den Heuvel MP and Yeo BTT (2017) A Spotlight on Bridging Microscale and Macroscale Human Brain Architecture. *Neuron* 93:1248-1251.
- Hilgetag CC, Burns GA, O'Neil MA, Scannell JW and Young MP (2000) Anatomical connectivity defines the organization of clusters of cortical areas in the macaque monkey and the cat. *Philos. Trans. R. Soc. Lond. B* 355: 91-110.
- Humphries MD and Gurney K (2008) Network Small-World-Ness: A Quantitative Method for Determining Canonical Network Equivalence. *Plos One* 3: e0002051.
- Jhonson RA and Wischern DW (1998) Applied Multivariate Statistical Analysis. Prentice Hall, Upper Saddle River, New Jersey 4th ed. ISBN 0-13-834194-X
- Kaiser M (2011) A tutorial in connectome analysis: Topological and spatial features of brain networks. *NeuroImage* 57:892-907.
- Lameu EL, Borges FS, Borges RR, Iarosz KC, Caldas IL, Batista AM, Viana RL and Kurths J (2016) Suppression of phase synchronisation in network based on cat's brain. *Chaos* 26:043107.
- Lo CY, Wang PN, Chou KH, Wang J, He Y and CP Lin (2010) Diffusion tensor tractography reveals abnormal topological organization in structural cortical networks in Alzheimers disease. *J. Neurosci.* 30:16876-16885.
- Iturria-Medina Y, Canales-Rodríguez EJ, Melie-García L, Valdés-Hernández PA, Martínez-Montes E, Alemán-Gómez Y and Sánchez-Bornot JM. (2007) Characterizing brain anatomical connections using diffusion weighted MRI and graph theory. *Neuroimage* 36:645-660.
- Iturria-Medina Y, Sotero RC, Canales-Rodríguez EJ, Alemán-Gómez Y, Melie-García L (2008) Studying the human brain anatomical network via diffusion-weighted MRI and Graph Theory. *Neuroimage* 40:1064-1076.
- Kaiser HF (1974) *Psychometrika* 39:31. <https://doi.org/10.1007/BF02291575>
- Mori S, Crain BJ, Chacko VP and van Zijl PC (1999) Three-dimensional tracking of axonal projections in the brain by magnetic resonance imaging. *Ann. Neurol.* 45: 265269.
- Maruyama G (1998) Basics of Structural Equation Modeling. Thousand Oaks, Calif: SAGE Publications, Inc.
- Newman MEJ (2000) Models of the Small World. *J. Stat. Phys.* 101:819-841.
- Newman MEJ (2002) Assortative Mixing in Networks. *Phys. Rev. Lett.* 89: 208701.
- Newman MEJ (2003) The Structure and Function of Complex Networks. *SIAM Rev.* 45:167-256.
- Newman MEJ and Girvan M (2003) Finding and evaluating community structure in networks. *Phys. Rev. E* 026113:1-15.
- Newman MEJ (2006) Modularity and community structure in networks. *P. Natl. Acad. Sci. USA* 103:8577-8582.
- Opsahl T and Panzarasa P (2009) Clustering in weighted networks. *Soc. Networks* 31:155-163.
- Opsahl T, Agneessens F and Skvoretz J (2010) Node centrality in weighted networks: Generalizing degree and shortest paths. *Soc. Networks* 32:245-251.
- Pol HH and Bullmore E (2013) Neural networks in psychiatry. *Eur. Neuropsychopharmacol.* 23:1-6.
- R Core Team (2018) R: A Language and Environment for Statistical Computing. R Foundation for Statistical Computing. Vienna, Austria. 2008. URL: <http://www.R-project.org/>
- Reijneveld JC, Ponten SC, Berendse HW and Stam CJ (2007) The application of graph theoretical analysis to complex networks in the brain. *Clin. Neurophysiol.* 118:2317-2331.
- Rubinov M and Sporns O (2010) Complex network measures of brain connectivity: uses and interpretations. *Neuroimage* 52:1059-1069.
- Sporns O and Zwi JD (2004) The small world of the cerebral cortex. *Neuroinformatics* 2:145-162.
- Sporns O, Tononi G and Kötter R (2005) The Human Connectome: A Structural Description of the Human Brain. *PLOS Comput. Biol.* 1:e42.
- Sporns O (2013) Structure and function of complex brain networks. *Dialogues Clin. Neurosci.* 15:247-262.
- Schank T and Wagner D (2005) Approximating Clustering-Coefficient and Transitivity. *J. Graph Algorithms Appl.* 9:265-275.
- Stam CJ, Jones BF, Nolte G, Breakspear M and Scheltens P (2007) Small-World Networks and Functional Connectivity in Alzheimers Disease. *Cereb. Cortex* 17:92-99.
- Stam CJ and Reijneveld JC (2007) Graph theoretical analysis of complex networks in the brain. *Nonlinear Biomed. Phys.* 1:3.
- Stam CJ and van Straaten EC (2012) The organization of physiological brain networks. *Clin. Neurophysiol.* 123: 1067-1087.

- Stam CJ (2014) Modern network science of neurological disorders. *Nat. Rev. Neurosci.* 15:683-695.
- Stoop R, Saase V, Wagner C, Stoop B and Stoop R (2013) Beyond Scale-Free Small-World Networks: Cortical Columns for Quick Brains. *Phys. Rev. Lett.* 110:108105.
- Tzourio-Mazoyer N, Landeau B, Papathanassiou D, Crivello F, Etard O, Delcroix N, Mazoyer B and Joliot M (2002) Automated anatomical labeling of activations in SPM using a macroscopic anatomical parcellation of the MNI MRI single-subject brain. *Neuroimage* 15:273289.
- Varshney LR, Chen BL, Paniagua E, Hall DH and Chklovskii DB (2011) Structural Properties of the *Caenorhabditis Elegans* Neuronal Network. *PLOS Comp. Biol.* 7:e1001066.
- Watts DJ and Strogatz SH (1998) Collective dynamics of small-world networks. *Nature* 393:440-442.
- Weisstein EW (2019) Adjacency Matrix. From MathWorld—A Wolfram Web Resource. <http://mathworld.wolfram.com/AdjacencyMatrix.html>
- White JG, Southgate E, Thomson JN and Brenner S (1986) The structure of the nervous system of the nematode *Caenorhabditis Elegans*. *Philos. Trans. Royal Soc. Lond. B* 314:1-340.
- Yao Z, Zhang Y, Lin L, Zhou Y, Xu C and Jiang T (2010) Abnormal Cortical Networks in Mild Cognitive Impairment and Alzheimers Disease. *PLOS Comp. Bio.* 6:e1001006.
- Zalesky A, Fornito A, Seal ML, Cocchi L, Westin CF, Bullmore ET, Egan GF and Pantelis C (2011) Disrupted Axonal Fiber Connectivity in Schizophrenia. *Biol. Psychiatry* 69:80-89.